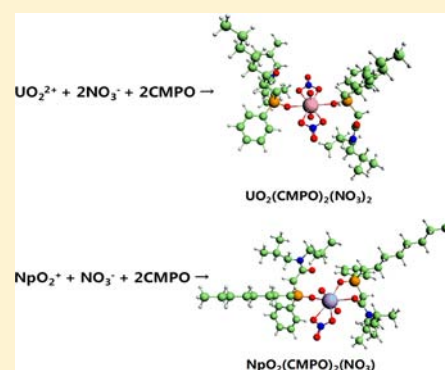


Density Functional Theory Studies of  $\text{UO}_2^{2+}$  and  $\text{NpO}_2^+$  Complexes with Carbamoylmethylphosphine Oxide LigandsCong-Zhi Wang,<sup>†</sup> Jian-Hui Lan,<sup>†</sup> Yu-Liang Zhao,<sup>†</sup> Zhi-Fang Chai,<sup>†</sup> Yue-Zhou Wei,<sup>‡</sup> and Wei-Qun Shi<sup>\*†</sup><sup>†</sup>Nuclear Energy Nano-Chemistry Group, Key Laboratory of Nuclear Analytical Techniques and Key Laboratory For Biomedical Effects of Nanomaterials and Nanosafety, Institute of High Energy Physics, Chinese Academy of Sciences, Beijing 100049, China<sup>‡</sup>Department of Nuclear Fuel Cycle and Material, School of Nuclear Science and Engineering, Shanghai Jiao Tong University, Shanghai 200240, China

## Supporting Information

**ABSTRACT:** The  $\text{UO}_2^{2+}$  and  $\text{NpO}_2^+$  extraction complexes with *n*-octyl(phenyl)-*N,N*-diisobutylmethylcarbamoyl phosphine oxide (CMPO) and diphenyl-*N,N*-diisobutylmethylcarbamoyl phosphine oxide ( $\text{Ph}_2\text{CMPO}$ ) have been investigated by density functional theory (DFT) in conjunction with relativistic small-core pseudopotentials. For these extraction complexes, especially the complexes of 2:1 (ligand/metal) stoichiometry,  $\text{UO}_2^{2+}$  and  $\text{NpO}_2^+$  predominantly coordinate with the phosphoric oxygen atoms. The CMPO and  $\text{Ph}_2\text{CMPO}$  ligands have higher selectivity for  $\text{UO}_2^{2+}$  over  $\text{NpO}_2^+$ , and for all of the extraction complexes, the metal–ligand interactions are mainly ionic. In most cases, the complexes with CMPO and  $\text{Ph}_2\text{CMPO}$  ligands have comparable metal–ligand binding energies, that is, the substitution of a phenyl ring for the *n*-octyl group at the phosphoryl group of CMPO has no obvious influence on the extraction of  $\text{UO}_2^{2+}$  and  $\text{NpO}_2^+$ . Moreover, hydration energies might play an important role in the extractability of CMPO and  $\text{Ph}_2\text{CMPO}$  for these actinyl ions.



## 1. INTRODUCTION

With the development of the economy, nuclear power plants are becoming principal sources of electric power. However, a large amount of spent nuclear fuel containing high radioactivity is being produced as a result. Safe treatment and disposal of the radioactive waste, especially high-level liquid waste (HLLW), which is the raffinate from the PUREX (plutonium uranium extraction) process, have become the key factors affecting the sustainable development of nuclear energy. Because HLLW contains large amounts of long-lived minor actinides together with fission products, selective extraction of the long-lived actinides from HLLW has received extensive attention throughout the world.

Neutral bidentate organophosphorous reagents such as carbamoylmethylphosphine oxides are considered to be efficient extractants for actinides extraction from HLLW and have been extensively investigated experimentally.<sup>1,2</sup> Because of the difference in the electronegativities and electron-donating abilities between the carbonyl and phosphoric oxygen atoms, the predominant coordinating group with actinide cations is the phosphoric oxygen. The carbonyl oxygen, owing to its weak ability to coordinate the actinide cation, can combine with a proton and act as an internal buffer.<sup>3</sup> Among these bidentate organophosphorous reagents, *n*-octyl(phenyl)-*N,N*-diisobutylmethylcarbamoyl phosphine oxide (CMPO) (Figure 1), which is used in the so-called TRUEX (transuranium extraction) process, was found to exhibit excellent extracting ability for actinide cations in acidic media.<sup>4–6</sup>

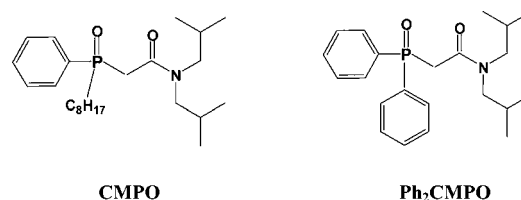


Figure 1. Structures of CMPO and  $\text{Ph}_2\text{CMPO}$ .

Many experimental studies on the liquid–liquid extraction of actinides with CMPO have been carried out for several decades. For instance, Horwitz and Kalina<sup>7</sup> reported the extraction of Am(III) from  $\text{HNO}_3$  solutions using a mixture of CMPO and tributyl phosphate (TBP) as the extractant and diethylbenzene, decalin, and normal aliphatic hydrocarbons as the diluents. They found that addition of TBP to CMPO can increase the extractability of Am(III) and improve phase compatibility. Mathur et al.<sup>8</sup> studied the extraction behavior of Am(III), Pu(IV), and U(VI) with a mixture of CMPO and TBP in dodecane. Hatakeyama et al.<sup>9</sup> investigated the structure of uranyl nitrate complex with CMPO in the solid state and in nonaqueous solvents without free CMPO using infrared (IR) and  $^{13}\text{C}$  and  $^{31}\text{P}$  NMR spectroscopies, and concluded that the uranyl nitrate complex with CMPO in both states has the same structure with two bidentate nitrate group and one bidentate

Received: July 20, 2012

Published: December 11, 2012

CMPO moiety distributed around the equatorial plane of uranyl ion, that is,  $\text{UO}_2(\text{NO}_3)_2(\text{CMPO})$ . Horwitz et al.<sup>10</sup> also studied the extraction of U(VI) with CMPO based on the conventional aqueous nitric acid/dodecane-based system and suggested that two monodentate CMPO molecules (P=O bind) as well as two bidentate nitrate anions coordinate to the linear  $\text{UO}_2^{2+}$ , forming a neutral, hexagonal bipyramidal complex, namely,  $\text{UO}_2(\text{NO}_3)_2(\text{CMPO})_2$ . Recently, the structures of these complexes were confirmed by extended X-ray absorption fine structure (EXAFS) studies.<sup>11</sup> Suzuki and co-workers<sup>12</sup> examined the extraction behavior of Np(V) from nitric acid solution by CMPO in the presence and absence of TBP using decalin and *n*-dodecane as the diluents and predicted that Np(V) could be extracted by CMPO through the extraction equation  $\text{NpO}_2^+ + \text{NO}_3^- + 2\text{CMPO} \rightarrow \text{NpO}_2(\text{NO}_3)(\text{CMPO})_2$ . In addition, they also studied the extraction of Np(V) from nitric acid solutions containing U(VI) by CMPO and confirmed that the distribution ratio of Np(V) increased because of the formation of the cation–cation complex of Np(V)–U(VI) in CMPO solution.<sup>13</sup>

In addition, another organophosphorous reagent, namely, diphenyl-*N,N*-diisobutylcarbamoyl phosphine oxide ( $\text{Ph}_2\text{CMPO}$ ) (Figure 1), was extensively studied in Russia.<sup>14–16</sup>

It was found that  $\text{Ph}_2\text{CMPO}$  is also efficient for actinides extraction and shows less tendency toward third-phase formation than CMPO.

Although there have been numerous experimental studies on the extractabilities of actinides by CMPO and  $\text{Ph}_2\text{CMPO}$ , many unclear scientific issues still remain, for example, the structures of the extracted complexes, the origin of the selectivity, and the corresponding thermodynamics and kinetics. Thus, computational studies are essential for explaining the complex behavior of these actinide species. However, to the best of our knowledge, only one theoretical report has been published that mainly focuses on the extraction complexes of  $\text{UO}_2^{2+}$  with CMPO in ionic liquid by molecular dynamics simulation.<sup>17</sup> That work compared the uranyl–CMPO complexes in dry and humid forms of the [BMI][PF<sub>6</sub>] ionic liquid and suggested that humidity is very important for the solvation of the free CMPO ligand and its complexes. In the present work, a theoretical study was carried out on the extraction of  $\text{UO}_2^{2+}$  and  $\text{NpO}_2^+$  from  $\text{HNO}_3$  solutions with CMPO and  $\text{Ph}_2\text{CMPO}$  using relativistic quantum mechanical (QM) calculations. We mainly concentrate on the equilibrium geometries and bonding nature, as well as the relative stability of the extraction complexes with CMPO and  $\text{Ph}_2\text{CMPO}$ . In addition, the solvent effects are also taken into account using the COSMO (conductor-like screening model) approach.<sup>18</sup>

## 2. THEORETICAL METHODS

Electron correlation effects were included by employing density functional theory (DFT) methods,<sup>19–22</sup> which have evolved as a practical and effective computational tool for medium to large actinide compounds.<sup>23–25</sup> Calculations were performed using the B3LYP functional, which is a hybrid Hartree–Fock (HF)/DFT method incorporating Becke's three-parameter functional (B3)<sup>26</sup> with the Lee, Yang, and Parr (LYP)<sup>27</sup> correlation functional.

The basis sets were analogous to those used in our previous studies.<sup>28–30</sup> For the U and Np atoms, relativistic effects were considered with the quasirelativistic effective core potentials (RECPs) and the associated valence basis sets developed by the Stuttgart and Dresden groups.<sup>31–33</sup> The adopted small-core RECPs include 60 electrons in the core for U and Np, whereas for the light atoms H, C, N, O, and P, the polarized all-electron 6-31G(d) basis sets were used

for geometry optimizations. It has been shown that the main features of actinide complexes can be accurately reproduced at this level of theory.<sup>34–36</sup> All of these computations were carried out with the Gaussian 03 program.<sup>37</sup>

Based on the optimized structures, the minimum character of the optimized structures was checked by frequency analysis at the B3LYP/6-311G(d,p)/RECP level of theory. The fine grid (75, 302) was the default in the Gaussian 03 code for evaluating integrals numerically.<sup>38</sup> Moreover, the finer grid (99, 590) in the Gaussian 09 code<sup>39</sup> was used for more precise resolution of the small imaginary vibrational frequencies. All of the species studied in this work exhibited real vibrational frequencies, indicating that these optimized structures correspond to minima on the potential energy surfaces. In addition, all of the predicted structures had negligible spin contamination in the unrestricted DFT ground states, with  $\langle S^2 \rangle$  values very close to the ideal value of  $S(S + 1)$ .

Geometry optimizations and electronic calculations for all of the species were carried out in the gas phase at the B3LYP/6-31G(d)/RECP level of theory. The natural atomic charges and Wiberg bond indices (WBIs)<sup>40</sup> were determined by natural bond orbital (NBO) analysis<sup>41–44</sup> at the same level of theory. The enthalpies (*H*), entropies (*S*), and Gibbs free energies (*G<sub>g</sub>*) were calculated with zero-point-energy (ZPE) and thermal corrections with the B3LYP/6-311G(d,p)/RECP method in the gas phase (298.15 K, 0.1 MPa). Based on the optimized structures, the solvation Gibbs free energies (*G<sub>sol</sub>*) were obtained by addressing bulk solvation effects with the COSMO approach<sup>18</sup> at the B3LYP/6-311G(d,p)/RECP level of theory. All solution-phase calculations were carried out in water. The default atomic radii in the Gaussian 03 code were used in the calculations. Because of the large molecular systems, only the gas-phase Gibbs free energies (*G<sub>g</sub>*) for 2:1 (ligand/metal) stoichiometric complexes were calculated in this work.

## 3. RESULTS AND DISCUSSION

To check the reliability of our theoretical methods, uranyl pentahydrate  $[\text{UO}_2(\text{H}_2\text{O})_5]^{2+}$  and uranyl nitrate dihydrate  $\text{UO}_2(\text{NO}_3)_2(\text{H}_2\text{O})_2$  were selected as theoretical models, and their geometries were also optimized in the gas phase using the exchange correlation functional BP86<sup>45,46</sup> with the same RECPs and basis sets (Figure 2).

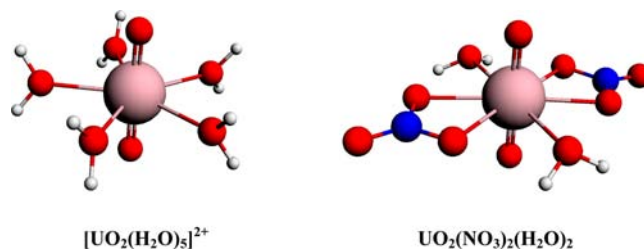


**Figure 2.** Optimized structures of  $[\text{UO}_2(\text{H}_2\text{O})_5]^{2+}$  and  $\text{UO}_2(\text{NO}_3)_2(\text{H}_2\text{O})_2$ . Red, white, blue, and light pink spheres represent O, H, N, and U, respectively.

The application of the B3LYP and BP86 methods led to  $C_5$  symmetry for the lowest-energy structure of  $[\text{UO}_2(\text{H}_2\text{O})_5]^{2+}$ , whereas the global minimum predicted for  $\text{UO}_2(\text{NO}_3)_2(\text{H}_2\text{O})_2$  was a  $C_{2v}$  trans structure. As reported in Table 1, the bond distances between the central metal atoms and the oxygen atoms for all of these species calculated by the B3LYP and BP86 methods were almost identical, as the average differences were about 0.02 Å. In view of the geometries optimized in the gas phase, the deviation of bond distances probably comes from the higher-symmetry structures. Moreover, compared with the available experimental data obtained using EXAFS measurements,<sup>47,48</sup> the B3LYP method predicted rather similar

**Table 1.** Selected Average Bond Lengths (Å) for  $[\text{UO}_2(\text{H}_2\text{O})_5]^{2+}$  and  $\text{UO}_2(\text{NO}_3)_2(\text{H}_2\text{O})_2$  Calculated by the B3LYP and BP86 Methods<sup>a</sup> in Comparison with Available Experimental Data (in Parentheses)<sup>b,c</sup>

	U=O	U—O(H <sub>2</sub> O)	U—O(NO <sub>3</sub> <sup>-</sup> )	average error
$[\text{UO}_2(\text{H}_2\text{O})_5]^{2+}$	1.753/1.775 (1.76)	2.484/2.472 (2.41)	— —	0.04/0.04
$\text{UO}_2(\text{NO}_3)_2(\text{H}_2\text{O})_2$	1.772/1.796 (1.754 ± 0.004)	2.539/2.546 (2.457 ± 0.004)	2.474/2.468 (2.510)	0.04/0.06

<sup>a</sup>.../... refers to the results obtained by the B3LYP and BP86 methods, respectively. <sup>b</sup>Experimental data for  $[\text{UO}_2(\text{H}_2\text{O})_5]^{2+}$  from ref 47. <sup>c</sup>Experimental data for  $\text{UO}_2(\text{NO}_3)_2(\text{H}_2\text{O})_2$  from ref 48.

structural parameters (average error of 0.04 Å). Therefore, the B3LYP results are taken into account in the following discussion.

**3.1.  $\text{UO}_2^{2+}$  and  $\text{NpO}_2^+$  Complexes in Aqueous Solution.** The structures and thermodynamics of the actinyl complexes in aqueous solution have been studied both by experimental and theoretical methods.<sup>47,49</sup> These studies concluded that pentacoordination is the most favorable structure for the uranyl and neptunyl ions in aqueous solution. As listed in Table 2, for both  $\text{UO}_2^{2+}$  and  $\text{NpO}_2^+$  in the gas

**Table 2.** Individual Energy Component Contributions (kcal/mol) for the Reactions of  $\text{UO}_2^{2+}$  and  $\text{NpO}_2^+$  in the Gas Phase (298.15 K, 0.1 MPa) and Changes in the Gibbs Free Energy (kcal/mol) for the Reactions in Aqueous Solution

reaction	$\Delta H$	$T\Delta S$	$\Delta G_g$	$\Delta G_{\text{sol}}$
$[\text{UO}_2(\text{H}_2\text{O})_6]^{2+} \rightarrow [\text{UO}_2(\text{H}_2\text{O})_5]^{2+} + \text{H}_2\text{O}$	16.7	10.0	6.7	-7.4
$[\text{NpO}_2(\text{H}_2\text{O})_6]^+ \rightarrow [\text{NpO}_2(\text{H}_2\text{O})_5]^+ + \text{H}_2\text{O}$	18.8	10.0	8.8	-8.4
$[\text{UO}_2(\text{H}_2\text{O})_5]^{2+} + \text{NO}_3^- \rightarrow [\text{UO}_2(\text{NO}_3)(\text{H}_2\text{O})_3]^+ + 2\text{H}_2\text{O}$	-179.3	9.5	-188.8	-11.5
$[\text{NpO}_2(\text{H}_2\text{O})_5]^+ + \text{NO}_3^- \rightarrow [\text{NpO}_2(\text{NO}_3)(\text{H}_2\text{O})_3] + 2\text{H}_2\text{O}$	-98.9	9.5	-108.4	-7.6
$[\text{UO}_2(\text{H}_2\text{O})_5]^{2+} + \text{NO}_3^- \rightarrow [\text{UO}_2(\text{NO}_3)_2(\text{H}_2\text{O})_2] + \text{H}_2\text{O}$	-196.1	-2.0	-194.2	-9.2
$[\text{NpO}_2(\text{H}_2\text{O})_5]^+ + \text{NO}_3^- \rightarrow [\text{NpO}_2(\text{NO}_3)_2(\text{H}_2\text{O})_2] + \text{H}_2\text{O}$	-115.0	-0.9	-114.2	-0.1
$[\text{UO}_2(\text{H}_2\text{O})_5]^{2+} + 2\text{NO}_3^- \rightarrow \text{UO}_2(\text{NO}_3)_2(\text{H}_2\text{O})_2 + 3\text{H}_2\text{O}$	-308.7	6.9	-315.7	-26.2
$[\text{NpO}_2(\text{H}_2\text{O})_5]^+ + 2\text{NO}_3^- \rightarrow [\text{NpO}_2(\text{NO}_3)_2(\text{H}_2\text{O})_2]^- + 3\text{H}_2\text{O}$	-131.8	8.0	-139.8	-16.4

phase, the changes in the Gibbs free energy,  $\Delta G_g$  for the reaction of hexahydrate to pentahydrate are all positive, indicating that  $\text{UO}_2^{2+}$  and  $\text{NpO}_2^+$  seem to prefer the hexahydrate. However, the changes in the Gibbs free energy in aqueous solution,  $\Delta G_{\text{sol}}$  show that the penta-aquo complexes,  $[\text{UO}_2(\text{H}_2\text{O})_5]^{2+}$  and  $[\text{NpO}_2(\text{H}_2\text{O})_5]^+$ , appear to be energetically favorable. Moreover, there are clearly large entropy contributions to the gas-phase free energy changes for these reactions.

Given that the  $\text{UO}_2^{2+}$  and  $\text{NpO}_2^+$  complexes studied here are charged species, we also carefully tested the influence of explicit water molecules in the second coordination sphere on the complexing reaction. It has been reported that, for some neutral and ionic organic species, the conductorlike polarizable continuum model (CPCM) with the UAKS cavities can provide the aqueous solvation free energies in best agreement with experimental data,<sup>50</sup> whereas COSMO is a reliable and stable continuum solvation model that appears to be more accurate for calculating the free energy in solvation of actinide species.<sup>18,51</sup> Thus, the continuum solvation models CPCM

(with the UAKS cavity) and COSMO were adopted (Table S1 in the Supporting Information). According to our calculations, the two solvation methods give consistent general trends, for example, the changes in the Gibbs free energy are all negative. In addition, the reaction trends for the cases studied here were not changed by taking into account the second coordination spheres of actinide ions. Based on our calculations, the CPCM (with the UAKS cavity) and COSMO solvation methods give relatively reliable results for calculating reaction energies involving charged  $\text{UO}_2^{2+}$  and  $\text{NpO}_2^+$  complexes. Actually, a previous investigation<sup>52</sup> also found that the solvation effects are represented accurately enough by these continuum solvation models with the first coordination sphere and that explicit inclusion of waters in the second coordination sphere has a modest influence on the energetics. In terms of the above discussion, we chose the COSMO model for further studying the actinyl aquo complexes and the extraction complexes with CMPO and  $\text{Ph}_2\text{CMPO}$ .

In the presence of nitrate ions (Table 2),  $\text{UO}_2^{2+}$  and  $\text{NpO}_2^+$  prefer to coordinate with the nitrate ions acting as bidentate ligands in both the gas phase and aqueous solution. As shown in Table 2, the changes in enthalpy are between -98.9 and -308.7 kcal/mol and represent the main contributions to the changes in the Gibbs free energy. According to the changes in the Gibbs free energy, the uranyl and neptunyl nitrate hydrates are more stable than  $[\text{UO}_2(\text{H}_2\text{O})_5]^{2+}$  and  $[\text{NpO}_2(\text{H}_2\text{O})_5]^+$ , respectively, suggesting that nitrate ions have stronger coordination ability than water molecules. As for the uranyl nitrate hydrates, the neutral  $\text{UO}_2(\text{NO}_3)_2(\text{H}_2\text{O})_2$  complex is more favorable energetically than the charged uranyl hydrates, suggesting that the electrostatic interaction significantly affects the stability of these U(VI) species. However, for the neptunyl nitrate hydrates, the charged  $[\text{NpO}_2(\text{NO}_3)_2(\text{H}_2\text{O})_2]^-$  complex is more favorable than the neutral complexes in the gas phase and aqueous solution, which indicates a more stable neutral neptunyl nitrate hydrate might exist. In fact, the neutral  $(\text{NpO}_2)_2(\text{NO}_3)_2(\text{H}_2\text{O})_5$  complex has been isolated already, and its structure has been identified by X-ray scattering.<sup>53</sup> Furthermore, although the tetrahydrates  $[\text{UO}_2(\text{NO}_3)(\text{H}_2\text{O})_4]^+$  and  $\text{NpO}_2(\text{NO}_3)(\text{H}_2\text{O})_4$  seem to be more stable than the corresponding trihydrates in the gas phase, the trihydrates are preferable when solvent effects are taken into account. This suggests that, in aqueous solution, steric interactions might also play an important role in the formation of the uranyl and neptunyl nitrate hydrates.

**3.2. Extraction Complexes with 1:1 (Ligand/Metal) Stoichiometry.** **3.2.1. Geometric Structures.** All possible complexes of  $\text{UO}_2^{2+}$  and  $\text{NpO}_2^+$  with a 1:1 CMPO/ $\text{Ph}_2\text{CMPO}$ -to-metal stoichiometry were predicted at the B3LYP/6-31G(d)/RECP level of theory. As shown in Figure 3 and Figure S1 (Supporting Information), for all of these species, CMPO and  $\text{Ph}_2\text{CMPO}$  are coordinated as bidentate chelating



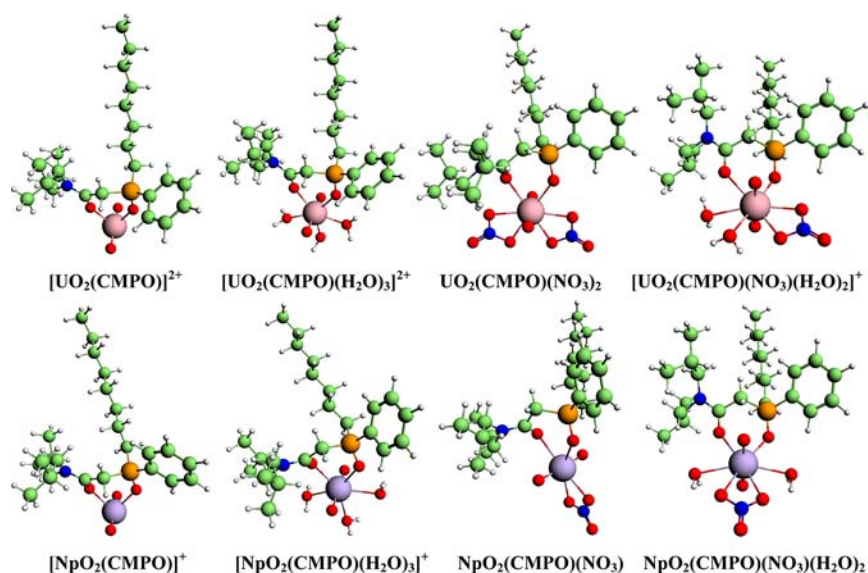


**Figure 3.** Optimized structures of the uranyl and neptunyl complexes with CMPO (1:1 type). Green, white, red, blue, orange, light pink, and light purple spheres represent C, H, O, N, P, U, and Np, respectively.

**Table 3.** U—O Bond Lengths (Å) for the Complexes of  $\text{UO}_2^{2+}$ ,  $\text{NpO}_2^+$ , and L (L = CMPO,  $\text{Ph}_2\text{CMPO}$ ) Calculated by the B3LYP Method<sup>a</sup>

species	An—O <sub>C</sub>	An—O <sub>P</sub>	An—O(NO <sub>3</sub> <sup>-</sup> ) <sup>b</sup>	An—O(H <sub>2</sub> O) <sup>b</sup>
[UO <sub>2</sub> L] <sup>2+</sup>	2.221/2.221	2.177/2.175	—	—
[UO <sub>2</sub> L(H <sub>2</sub> O) <sub>3</sub> ] <sup>2+</sup>	2.339/2.339	2.314/2.315	—	2.529/2.528
UO <sub>2</sub> L(NO <sub>3</sub> ) <sub>2</sub>	2.578/2.528	2.452/2.459	2.488/2.489	—
[UO <sub>2</sub> L(NO <sub>3</sub> )(H <sub>2</sub> O) <sub>2</sub> ] <sup>+</sup>	2.662/2.494	2.347/2.444	2.453/2.572	2.626/2.491
[NpO <sub>2</sub> L] <sup>+</sup>	2.382/2.377	2.359/2.342	—	—
[NpO <sub>2</sub> L(H <sub>2</sub> O) <sub>3</sub> ] <sup>+</sup>	2.479/2.460	2.520/2.504	—	2.606/2.588
NpO <sub>2</sub> L(NO <sub>3</sub> )	2.578/2.518	2.490/2.505	2.481/2.477	—
NpO <sub>2</sub> L(NO <sub>3</sub> )(H <sub>2</sub> O) <sub>2</sub>	2.616/2.623	2.551/2.565	2.599/2.607	2.717/2.706

<sup>a</sup>.../... refers to the results for CMPO and  $\text{Ph}_2\text{CMPO}$  complexes, respectively. <sup>b</sup>An—O average bond lengths.

**Table 4.** Wiberg Bond Indices (WBIs) of An—O Bonds and Natural Charges on the An and O Atoms for the Complexes of  $\text{UO}_2^{2+}$ ,  $\text{NpO}_2^+$ , and L (L = CMPO,  $\text{Ph}_2\text{CMPO}$ ) Obtained by the B3LYP Method<sup>a</sup>

species	An—O <sub>C</sub>	An—O <sub>P</sub>	Q(An)	Q(O <sub>C</sub> )	Q(O <sub>P</sub> )
[UO <sub>2</sub> L] <sup>2+</sup>	0.393/0.391	0.475/0.476	3.104/3.105	-0.840/-0.838	-1.166/-1.168
[UO <sub>2</sub> L(H <sub>2</sub> O) <sub>3</sub> ] <sup>2+</sup>	0.325/0.346	0.361/0.362	2.984/2.991	-0.785/-0.780	-1.154/-1.146
UO <sub>2</sub> L(NO <sub>3</sub> ) <sub>2</sub>	0.176/0.194	0.242/0.234	2.855/2.851	-0.707/-0.705	-1.107/-1.105
[UO <sub>2</sub> L(NO <sub>3</sub> )(H <sub>2</sub> O) <sub>2</sub> ] <sup>+</sup>	0.166/0.228	0.326/0.264	2.897/2.891	-0.749/-0.735	-1.117/-1.129
[NpO <sub>2</sub> L] <sup>+</sup>	0.172/0.176	0.197/0.181	2.602/2.627	-0.809/-0.810	-1.183/-1.184
[NpO <sub>2</sub> L(H <sub>2</sub> O) <sub>3</sub> ] <sup>+</sup>	0.157/0.179	0.147/0.154	2.506/2.471	-0.763/-0.742	-1.171/-1.159
NpO <sub>2</sub> L(NO <sub>3</sub> )	0.112/0.125	0.138/0.135	2.551/2.534	-0.749/-0.733	-1.152/-1.143
NpO <sub>2</sub> L(NO <sub>3</sub> )(H <sub>2</sub> O) <sub>2</sub>	0.117/0.123	0.141/0.140	2.436/2.427	-0.702/-0.695	-1.118/-1.123

<sup>a</sup>.../... refers to the results for CMPO and  $\text{Ph}_2\text{CMPO}$  complexes, respectively.

ligands through carbonyl and phosphoric oxygen donor atoms. Moreover, the substituents of these ligands (CMPO and  $\text{Ph}_2\text{CMPO}$ ) have small effect on the geometrical structures of the formed species, except for  $[\text{UO}_2\text{L}(\text{NO}_3)(\text{H}_2\text{O})_2]^+$  with differences in the An—O bond lengths of less than 0.17 Å (Table 3).

It should be noted that, although the ionic radii of  $\text{U}^{6+}$  (0.73 Å) and  $\text{Np}^{5+}$  (0.75 Å) are very close to each other, the An—O bond lengths in  $[\text{UO}_2\text{L}]^{2+}$  and  $[\text{UO}_2\text{L}(\text{H}_2\text{O})_3]^{2+}$  are about 0.16 Å shorter than those in  $[\text{NpO}_2\text{L}]^+$  and  $[\text{NpO}_2\text{L}(\text{H}_2\text{O})_3]^+$ , respectively. Moreover, the An—O bond lengths of the U(VI) nitrate complexes are almost smaller than those of the Np(V)

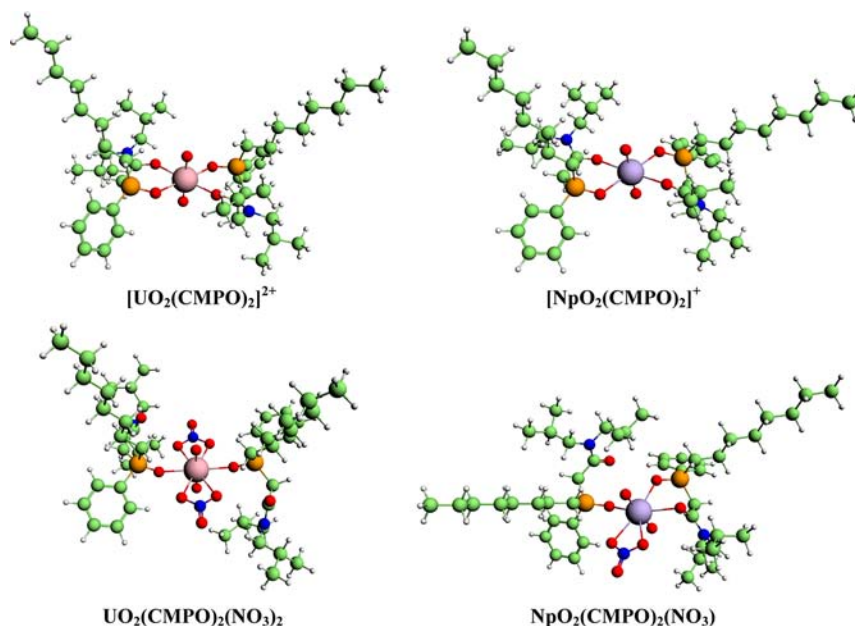
complexes. These results indicate that the interactions between the metal atoms and the ligands for the U(VI) species are much stronger than those for the Np(V) species, that is, the extractability of CMPO and  $\text{Ph}_2\text{CMPO}$  for  $\text{NpO}_2^+$  is much lower than that for  $\text{UO}_2^{2+}$ , which has been already confirmed by experiments.<sup>54</sup>

**3.2.2. NBO Analysis.** To provide insight into the bonding nature of these extraction complexes, NBO analysis was performed at the B3LYP/6-31G(d)/RECP level of theory. As shown in Table 4, the WBIs of the An—O bonds for all of these complexes are in the range of 0.1–0.5, indicating that the interactions between the metal atom and ligand are

**Table 5.** Changes in Enthalpy, Entropy, and Binding Energies (kcal/mol) for the Complexes of  $\text{UO}_2^{2+}$ ,  $\text{NpO}_2^+$ , and L (L = CMPO,  $\text{Ph}_2\text{CMPO}$ ) Obtained by the B3LYP Method<sup>a</sup>

reaction	$\Delta H$	$T\Delta S$	$\Delta G_g$	$\Delta G_{\text{sol}}$
$\text{UO}_2^{2+} + \text{L} \rightarrow [\text{UO}_2\text{L}]^{2+}$	-228.4/-230.0	-11.9/-12.0	-216.5/-218.0	-72.3/-73.1
$\text{UO}_2^{2+} + \text{L} + 3\text{H}_2\text{O} \rightarrow [\text{UO}_2\text{L}(\text{H}_2\text{O})_3]^{2+}$	-323.8/-325.8	-42.3/-43.0	-281.4/-282.8	-101.6/-103.2
$\text{UO}_2^{2+} + \text{L} + 2\text{NO}_3^- \rightarrow \text{UO}_2\text{L}(\text{NO}_3)_2$	-569.3/-569.6	-35.0/-34.4	-534.3/-535.2	-123.6/-123.8
$\text{UO}_2^{2+} + \text{L} + \text{NO}_3^- + 2\text{H}_2\text{O} \rightarrow [\text{UO}_2\text{L}(\text{NO}_3)(\text{H}_2\text{O})_2]^+$	-482.0/-486.4	-45.0/-45.0	-437.0/-441.3	-106.9/-110.1
$\text{NpO}_2^+ + \text{L} \rightarrow [\text{NpO}_2\text{L}]^+$	-109.4/-111.2	-12.8/-11.8	-96.5/-99.4	-34.5/-40.1
$\text{NpO}_2^+ + \text{L} + 3\text{H}_2\text{O} \rightarrow [\text{NpO}_2\text{L}(\text{H}_2\text{O})_3]^+$	-162.4/-172.0	-41.4/-40.6	-121.0/-131.4	-51.4/-52.2
$\text{NpO}_2^+ + \text{L} + \text{NO}_3^- \rightarrow \text{NpO}_2\text{L}(\text{NO}_3)$	-226.4/-228.0	-21.5/-22.3	-204.9/-205.7	-60.4/-57.4
$\text{NpO}_2^+ + \text{L} + \text{NO}_3^- + 2\text{H}_2\text{O} \rightarrow \text{NpO}_2\text{L}(\text{NO}_3)(\text{H}_2\text{O})_2$	-256.3/-256.7	-42.2/-42.6	-214.1/-214.2	-56.5/-52.2

<sup>a</sup>.../... refers to the results for CMPO and  $\text{Ph}_2\text{CMPO}$  complexes, respectively.

**Figure 4.** Optimized structures of the uranyl and neptunyl complexes with CMPO (2:1 type). Green, white, red, blue, orange, light pink, and light purple spheres represent C, H, O, N, P, U, and Np, respectively.

predominantly ionic and that the electrostatic interaction dominates these bondings. Aside from  $[\text{UO}_2\text{L}(\text{NO}_3)(\text{H}_2\text{O})_2]^+$ , the WBIs of the An—O bonds for the extraction complexes of CMPO are nearly equal to those of  $\text{Ph}_2\text{CMPO}$ . This is in accordance with the An—O bond lengths for the CMPO and  $\text{Ph}_2\text{CMPO}$  complexes.

For the U(VI) complexes, all of the WBIs of the U—O<sub>C</sub> bonds are smaller than those of the U—O<sub>P</sub> bonds, which suggests that the U—O<sub>P</sub> bonds have a greater degree of covalent character. The same phenomenon was also observed for the Np(V) complexes except for  $[\text{NpO}_2\text{L}(\text{H}_2\text{O})_3]^+$ . This might be due to the existence of hydrogen-bonding interactions between the oxygen atom of the phosphoryl group and one of the water hydrogen atoms in  $[\text{NpO}_2\text{L}(\text{H}_2\text{O})_3]^+$ , which can be indicated by the O<sub>P</sub>—O<sub>H<sub>2</sub>O</sub> distance of 2.72 Å. In addition, the WBIs of the An—O<sub>C</sub> and An—O<sub>P</sub> bonds decrease when  $\text{UO}_2^{2+}$  and  $\text{NpO}_2^+$  coordinate to water molecules and nitrate ions; for example, for  $[\text{UO}_2\text{L}]^{2+}$ , the WBIs of the An—O<sub>C</sub> bond is about 0.39, whereas for  $\text{UO}_2\text{L}(\text{NO}_3)_2$ , it is about 0.18.

As reported in Table 4, on the basis of natural population analysis for the U(VI) and Np(V) complexes, the natural charges on the U atoms are larger than those on the Np atoms, which also suggests that CMPO and  $\text{Ph}_2\text{CMPO}$  have higher extractability for U(VI) than for Np(V). Furthermore, the

natural charges on the O atoms of the phosphoryl group are more negative than those of the carbonyl group, confirming that the phosphoric oxygen atoms of CMPO and  $\text{Ph}_2\text{CMPO}$  have stronger coordinating ability to the metal cations than the carbonyl oxygen atoms and that these extractants predominantly bind with the phosphoric oxygen atoms.

**3.2.3. Metal–Ligand Binding Energy.** Table 5 lists the changes in enthalpy, entropy, and binding energies for the metal–ligand complexation reactions. As presented in Table 5, the gas-phase reaction enthalpies were found to range from -109.4 to -569.6 kcal/mol, which are much more negative than the  $T\Delta S$ . This results in the relatively large negative gas-phase binding energies ( $\Delta G_g$ ), which are between -96.5 and -535.2 kcal/mol. In contrast, because of the solvent effects in aqueous solution, the hydration binding energies ( $\Delta G_{\text{sol}}$ ) are much lower than the corresponding gas-phase binding energies, ranging from -34.5 to -123.8 kcal/mol. This suggests that the solvation energy plays a significant role in the extraction process of the actinides with CMPO and  $\text{Ph}_2\text{CMPO}$ .

As expected, the gas-phase and hydration binding energies of the U(VI) complexes are more negative than those of the Np(V) complexes, which also confirms the experimental result that the extraction U(VI) complexes are more stable than the Np(V) complexes.<sup>54</sup> In most cases, the binding energies of

these actinyl complexes with Ph<sub>2</sub>CMPO are close to those of the corresponding complexes with CMPO, which suggests that CMPO and Ph<sub>2</sub>CMPO have comparable extractabilities for UO<sub>2</sub><sup>2+</sup> and NpO<sub>2</sub><sup>+</sup>.

**3.3. Extraction Complexes with 2:1 (Ligand/Metal) Stoichiometry.** **3.3.1. Geometric Structures.** At the B3LYP/6-31G(d)/RECP level of theory, for the charged complexes of 2:1 (ligand/metal) stoichiometry [UO<sub>2</sub>L<sub>2</sub>]<sup>2+</sup> and [NpO<sub>2</sub>L<sub>2</sub>]<sup>+</sup>, CMPO and Ph<sub>2</sub>CMPO are bidentate ligands (Figure 4 and Figure S2 in the Supporting Information). In contrast, for the neutral UO<sub>2</sub>L<sub>2</sub>(NO<sub>3</sub>)<sub>2</sub> complexes, the CMPO and Ph<sub>2</sub>CMPO ligands coordinate in monodentate fashion to uranyl through the phosphoric oxygen atom. At the same time, the two nitrate anions are coordinated to the U(VI) center as bidentate ligands forming a hexagonal bipyramidal structure, which is consistent with the EXAFS data for uranyl complexes in dodecane solutions.<sup>11</sup> However, each of the NpO<sub>2</sub>L<sub>2</sub>(NO<sub>3</sub>) complexes has one bidentate and one monodentate CMPO (or Ph<sub>2</sub>CMPO) ligands (P=O bind), as well as one bidentate nitrate anion coordinated to the NpO<sub>2</sub><sup>+</sup> moiety.

As shown in Table 6, for all of the 2:1-type complexes with different ligands, the bond lengths between the central metal

**Table 6. An—O Average Bond Lengths (Å) for the UO<sub>2</sub><sup>2+</sup> and NpO<sub>2</sub><sup>+</sup> Complexes with L (L = CMPO, Ph<sub>2</sub>CMPO) (2:1 Type) Calculated by the B3LYP Method<sup>a</sup> in Comparison with Available Experimental Data (in Parentheses)<sup>b</sup>**

	An—O <sub>C</sub>	An—O <sub>P</sub>	An—O(NO <sub>3</sub> <sup>-</sup> )
[UO <sub>2</sub> L <sub>2</sub> ] <sup>2+</sup>	2.354/2.356	2.321/2.326	—
[NpO <sub>2</sub> L <sub>2</sub> ] <sup>+</sup>	2.492/2.475	2.468/2.448	—
UO <sub>2</sub> L <sub>2</sub> (NO <sub>3</sub> ) <sub>2</sub>	—	2.413/2.406 (2.38 ± 0.02)	2.540/2.543 (2.53 ± 0.02)
NpO <sub>2</sub> L <sub>2</sub> (NO <sub>3</sub> )	2.633/2.547	2.464/2.492	2.551/2.544

<sup>a</sup>.../... refers to the results for CMPO and Ph<sub>2</sub>CMPO complexes, respectively. <sup>b</sup>Experimental data for UO<sub>2</sub>L<sub>2</sub>(NO<sub>3</sub>)<sub>2</sub> from ref 11.

atoms and the oxygen atoms of the ligands are very close to each other. For [UO<sub>2</sub>L<sub>2</sub>]<sup>2+</sup> and [NpO<sub>2</sub>L<sub>2</sub>]<sup>+</sup>, the An—O bond lengths are, on average, 0.1 Å longer than those for the corresponding 1:1 stoichiometric complexes [UO<sub>2</sub>L]<sup>2+</sup> and [NpO<sub>2</sub>L]<sup>+</sup>, mainly because of the spatial steric effects of the CMPO and Ph<sub>2</sub>CMPO ligands. As for the natural UO<sub>2</sub>L<sub>2</sub>(NO<sub>3</sub>)<sub>2</sub> and NpO<sub>2</sub>L<sub>2</sub>(NO<sub>3</sub>) complexes, the calculated An—O<sub>P</sub> bond lengths were found to be shorter than those of the corresponding 1:1-type complexes, suggesting that the bonds between the central metal atoms and the phosphoric oxygen atoms in these natural complexes are relatively strong. On the other hand, the calculated An—O bond lengths for UO<sub>2</sub>L<sub>2</sub>(NO<sub>3</sub>)<sub>2</sub> are in good agreement with the experimental results.<sup>11</sup>

**3.3.2. NBO Analysis.** The WBIs of the An—O<sub>C</sub> and An—O<sub>P</sub> bonds for the 2:1-type complexes are between 0.1 and 0.4

(Table 7), which are smaller than those for the corresponding 1:1-type complexes. This suggests that the ionic character of the metal—ligand bonds for the 2:1-type complexes is slightly weaker than that for the 1:1-type complexes, which is predominantly due to the steric interactions between the two CMPO (or Ph<sub>2</sub>CMPO) ligands.

Similar to the 1:1-type complexes, the WBIs of the An—O<sub>C</sub> and An—O<sub>P</sub> bonds for these 2:1-type complexes of CMPO are close to the values for the corresponding complexes of Ph<sub>2</sub>CMPO. The WBIs of the An—O<sub>P</sub> bonds are larger than those of the An—O<sub>C</sub> bonds, and the natural charges on the phosphoric oxygen atoms are more negative than those on the carbonyl oxygen atoms. Moreover, the natural charges on the U atoms are larger than those on the Np atoms. All of these results confirm that CMPO and Ph<sub>2</sub>CMPO have higher extractability for U(VI) than for Np(V)<sup>54</sup> and that, for all of these complexes, especially UO<sub>2</sub>L<sub>2</sub>(NO<sub>3</sub>)<sub>2</sub>, the phosphoric oxygen atoms have stronger coordinating ability to the metal cations than the carbonyl oxygen atoms.

**3.3.3. Stability.** To estimate the stability of these 2:1 (ligand/metal) stoichiometric complexes, the metal—ligand complexation reactions were investigated in the gas phase by the B3LYP method. The changes in enthalpy, entropy, and Gibbs free energy including ZPE and thermal corrections are listed in Table 8. Because the QM method has difficulty in calculating solvent effects for large systems, we present only the results for the gas phase here.

As shown in Table 8, the reaction enthalpies are distinctly exothermic, and the entropy has a small effect on the binding energies. In general, the binding energies for these 2:1-type complexes range from −130.9 to −540.4 kcal/mol, and all of these complexes with CMPO and Ph<sub>2</sub>CMPO ligands have comparable binding strengths. Similar to the 1:1-type complexes, the binding energies of the neutral UO<sub>2</sub>L<sub>2</sub>(NO<sub>3</sub>)<sub>2</sub> and NpO<sub>2</sub>L<sub>2</sub>(NO<sub>3</sub>) complexes are more negative than those of the charged [UO<sub>2</sub>L<sub>2</sub>]<sup>2+</sup> and [NpO<sub>2</sub>L<sub>2</sub>]<sup>+</sup> complexes. Thus, as reported in the literature,<sup>11,12</sup> UO<sub>2</sub><sup>2+</sup> and NpO<sub>2</sub><sup>+</sup> prefer to form 2:1-type neutral complexes in nitrate-rich acid solution, and the reaction of forming neutral complex studied here is probably one of the dominant complexing reactions. In addition, the binding energies of the UO<sub>2</sub><sup>2+</sup> complexes are more negative than those of the NpO<sub>2</sub><sup>+</sup> complexes, which is in agreement with the experimental observation<sup>54</sup> that the formation of UO<sub>2</sub><sup>2+</sup> complexes with CMPO and Ph<sub>2</sub>CMPO ligands is thermodynamically more favored than that of NpO<sub>2</sub><sup>+</sup> complexes.

Furthermore, the stability of the 2:1-type complexes was also investigated in the gas phase by a series of possible complexing reactions with the most stable actinyl hydrates and actinyl nitrate hydrates as well as the 1:1-type complexes (Table 9). In most cases, the changes in enthalpy were found to be negative, and the entropy contributions to the free energy were relatively large. According to the changes in the Gibbs free energy, the

**Table 7. Average Wiberg Bond Indices (WBIs) of An—O and Natural Charges on the U and O Atoms for the UO<sub>2</sub><sup>2+</sup> and NpO<sub>2</sub><sup>+</sup> Complexes with L (L = CMPO, Ph<sub>2</sub>CMPO) (2:1 Type) Calculated by the B3LYP Method<sup>a</sup>**

species	An—O <sub>C</sub>	An—O <sub>P</sub>	Q(An)	Q(O <sub>C</sub> )	Q(O <sub>P</sub> )
[UO <sub>2</sub> L <sub>2</sub> ] <sup>2+</sup>	0.292/0.279	0.337/0.317	3.008/3.010	−0.772/−0.781	−1.137/−1.136
[NpO <sub>2</sub> L <sub>2</sub> ] <sup>+</sup>	0.156/0.149	0.166/0.162	2.513/2.565	−0.739/−0.745	−1.149/−1.143
UO <sub>2</sub> L <sub>2</sub> (NO <sub>3</sub> ) <sub>2</sub>	—	0.281/0.269	2.855/2.853	—	−1.118/−1.111
NpO <sub>2</sub> L <sub>2</sub> (NO <sub>3</sub> )	0.116/0.135	0.171/0.156	2.450/2.481	−0.733/−0.724	−1.125/−1.128

<sup>a</sup>.../... refers to the results for CMPO and Ph<sub>2</sub>CMPO complexes, respectively.



**Table 8.** Calculated Changes in Enthalpy, Entropy, and Binding Energies (kcal/mol) for the  $\text{UO}_2^{2+}$  and  $\text{NpO}_2^+$  Complexes with L (L = CMPO,  $\text{Ph}_2\text{CMPO}$ ) (2:1 Type) in the Gas Phase (298.15 K, 0.1 MPa) Obtained by the B3LYP Method<sup>a</sup>

reaction	$\Delta H$	$T\Delta S$	$\Delta G_g$
$[\text{UO}_2]^{2+} + 2\text{L} \rightarrow [\text{UO}_2\text{L}_2]^{2+}$	-337.0/-337.8	-25.6/-25.8	-311.3/-312.0
$[\text{NpO}_2]^+ + 2\text{L} \rightarrow [\text{NpO}_2\text{L}_2]^+$	-160.9/-156.5	-23.7/-25.6	-137.3/-130.9
$[\text{UO}_2]^{2+} + 2\text{L} + 2\text{NO}_3^- \rightarrow \text{UO}_2\text{L}_2(\text{NO}_3)_2$	-589.1/-582.9	-48.7/-48.1	-540.4/-534.8
$[\text{NpO}_2]^+ + 2\text{L} + \text{NO}_3^- \rightarrow \text{NpO}_2\text{L}_2(\text{NO}_3)$	-240.4/-240.9	-34.7/-36.7	-205.7/-204.1

<sup>a</sup>.../... refers to the results for CMPO and  $\text{Ph}_2\text{CMPO}$  complexes, respectively.

**Table 9.** Calculated Changes in Enthalpy, Entropy, and Gibbs Free Energy (kcal/mol) for Complexing Reactions of  $\text{UO}_2^{2+}$  and  $\text{NpO}_2^+$  with L (L = CMPO,  $\text{Ph}_2\text{CMPO}$ ) (2:1 Type) in the Gas Phase (298.15 K, 0.1 MPa) Obtained by the B3LYP Method<sup>a</sup>

reaction	$\Delta H$	$T\Delta S$	$\Delta G_g$
$[\text{UO}_2(\text{H}_2\text{O})_5]^{2+} + 2\text{L} \rightarrow [\text{UO}_2\text{L}_2]^{2+} + 5\text{H}_2\text{O}$	-70.0/-70.9	24.0/23.9	-94.0/-94.7
$[\text{NpO}_2(\text{H}_2\text{O})_5]^+ + 2\text{L} \rightarrow [\text{NpO}_2\text{L}_2]^+ + 5\text{H}_2\text{O}$	-10.5/-6.1	24.9/23.0	-35.4/-29.0
$\text{UO}_2(\text{NO}_3)_2(\text{H}_2\text{O})_2 + 2\text{L} \rightarrow \text{UO}_2\text{L}_2(\text{NO}_3)_2 + 2\text{H}_2\text{O}$	-13.4/-7.3	-6.1/-5.4	-7.4/-1.8
$[\text{NpO}_2(\text{NO}_3)_2(\text{H}_2\text{O})_2]^- + 2\text{L} \rightarrow \text{NpO}_2\text{L}_2(\text{NO}_3) + \text{NO}_3^- + 2\text{H}_2\text{O}$	41.8/41.4	5.9/3.9	35.9/37.5
$\text{UO}_2\text{L}(\text{NO}_3)_2 + \text{L} \rightarrow \text{UO}_2\text{L}_2(\text{NO}_3)_2$	-19.8/-13.3	-13.7/-13.7	-6.1/0.4
$\text{NpO}_2\text{L}(\text{NO}_3) + \text{L} \rightarrow \text{NpO}_2\text{L}_2(\text{NO}_3)$	-14.1/-12.8	-13.3/-14.4	-0.8/1.6

<sup>a</sup>.../... refers to the results for CMPO and  $\text{Ph}_2\text{CMPO}$  complexes, respectively.

reactions for the uranyl and neptunyl hydrates forming the charged 2:1-type complexes were predicted to be endothermic, indicating that these reactions are favorable in the gas phase. However, the reaction  $[\text{NpO}_2(\text{NO}_3)_2(\text{H}_2\text{O})_2]^- + 2\text{L} \rightarrow \text{NpO}_2\text{L}_2(\text{NO}_3) + \text{NO}_3^- + 2\text{H}_2\text{O}$  was predicted to be exothermic by about 35.9 and 37.5 kcal/mol for L = CMPO and  $\text{Ph}_2\text{CMPO}$ , respectively, suggesting that it is unfavorable in the extraction process. As expected, for the U(VI) complexes, the changes in the Gibbs free energy of the complexing reactions were found to be more negative than those for the corresponding Np(V) complexes. Aside from the reaction  $[\text{UO}_2(\text{H}_2\text{O})_5]^{2+} + 2\text{L} \rightarrow [\text{UO}_2\text{L}_2]^{2+} + 5\text{H}_2\text{O}$ , for the U(VI) and Np(V) complexes with CMPO ligands, the changes in the Gibbs free energy of these complexing reactions were found to be more negative than those with  $\text{Ph}_2\text{CMPO}$  ligands, and the difference for the changes in the Gibbs free energy was 0.7–6.5 kcal/mol. These relatively small differences indicate that the substitution of a phenyl ring for the *n*-octyl group of CMPO has little influence on the extractability of  $\text{UO}_2^{2+}$  and  $\text{NpO}_2^+$ .

#### 4. SUMMARY AND CONCLUSIONS

In the present quantum chemical study, the equilibrium geometries, bonding natures, and stabilities of the  $\text{UO}_2^{2+}$  and  $\text{NpO}_2^+$  extraction complexes with CMPO and  $\text{Ph}_2\text{CMPO}$  were investigated using relativistic DFT calculations. For the 1:1-type extraction complexes, the CMPO and  $\text{Ph}_2\text{CMPO}$  ligands are coordinated as bidentate chelating ligands through the carbonyl oxygen and phosphoric oxygen atoms. Nevertheless, for the 2:1-type complexes, CMPO and  $\text{Ph}_2\text{CMPO}$  mainly coordinate to uranyl and neptunyl through the phosphoric oxygen atom. NBO analysis indicates that the bonding between the metal and the ligand is mainly ionic. For all of these extraction complexes, the phosphoric oxygen atoms of CMPO and  $\text{Ph}_2\text{CMPO}$  have stronger coordinating ability to the metal cations than the carbonyl oxygen atoms. According to the changes in the Gibbs free energy for the complexing reactions, CMPO and  $\text{Ph}_2\text{CMPO}$  have higher extractability for  $\text{UO}_2^{2+}$  than that for  $\text{NpO}_2^+$ , which agrees well with the experimental results. The presence of solvent probably plays a significant role in the extraction behavior of the actinyl ions with CMPO and  $\text{Ph}_2\text{CMPO}$ . For each of these complexes, the CMPO and

$\text{Ph}_2\text{CMPO}$  ligands have comparable metal–ligand binding strengths.

#### ■ ASSOCIATED CONTENT

##### § Supporting Information

Changes in the Gibbs free energy (kcal/mol) including zero-point energy (ZPE) and thermal corrections for the reactions concerning  $\text{UO}_2^{2+}$  and  $\text{NpO}_2^+$  in aqueous solution (Table S1). Structures of the uranyl and neptunyl complexes with  $\text{Ph}_2\text{CMPO}$  (1:1 and 2:1 types) optimized using the B3LYP method (Figures S1 and S2). This material is available free of charge via the Internet at <http://pubs.acs.org>.

#### ■ AUTHOR INFORMATION

##### Corresponding Author

\*E-mail: [shiwq@ihep.ac.c](mailto:shiwq@ihep.ac.c)

##### Notes

The authors declare no competing financial interest.

#### ■ ACKNOWLEDGMENTS

This work was supported by the National Natural Science Foundation of China (Grants 21101157, 11105162, and 21201166), the Major Research Plan “Breeding and Transmutation of Nuclear Fuel in Advanced Nuclear Fission Energy System” of the Natural Science Foundation of China (Grants 91026007 and 91126006), and the “Strategic Priority Research Program” of the Chinese Academy of Sciences (Grants XDA03010401 and XDA03010403). The results described in this work were obtained on the ScGrid of the Supercomputing Center, Computer Network Information Center of the Chinese Academy of Sciences.

#### ■ REFERENCES

- (1) Musikas, C.; Hubert, H. In *Proceedings of the International Solvent Extraction Conference*; American Institute of Chemical Engineers: New York, 1983; p 449.
- (2) Horwitz, E. P.; Schulz, W. W. In *Proceedings of the International Solvent Extraction Conference*; DECHEMA: Frankfurt am Main, 1986; p 81.
- (3) Danesi, P. R. In *Developments in Solvent Extraction*; Alegret, S., Ed.; Ellis Horwood Ltd.: Chichester, U.K., 1988; p 209.

- (4) Vandegrift, G. F.; Leonard, R. A.; Steindler, M. J.; Horwitz, E. P.; Basile, L. J.; Diamond, H.; Kalina, D. G.; Kaplan, L. *Transuranic Decontamination of Nitric Acid Solutions by the Truex Solvent Extraction Process-Preliminary Development Studies*; Report ANL-84-45; Argonne National Laboratory: Argonne, IL, 1984.
- (5) Horwitz, E. P.; Kalina, D. G.; Diamond, H.; Vandegrift, G. F.; Schulz, W. W. *Solvent Extr. Ion Exch.* **1985**, *3*, 75.
- (6) Horwitz, E. P.; Kalina, D. G.; Diamond, H.; Kaplan, L.; Vandegrift, G. F.; Leonard, R. A.; Steindler, M. J.; Schulz, W. W. German Patent DE85 010251, 1985.
- (7) Horwitz, E. P.; Kalina, D. G. *Solvent Extr. Ion Exch.* **1984**, *2*, 179.
- (8) Mathur, J. N.; Murali, M. S.; Natarajan, P. R. *Talanta* **1992**, *39*, 493.
- (9) Hatakeyama, K.; Park, Y.-Y.; Tomiyasu, H. *J. Nucl. Sci. Technol.* **1995**, *32*, 1146.
- (10) Horwitz, E. P.; Diamond, H.; Martin, K. A. *Solvent Extr. Ion Exch.* **1987**, *5*, 447.
- (11) Visser, A. E.; Jensen, M. P.; Laszak, I.; Nash, K. L.; Choppin, G. R.; Rogers, R. D. *Inorg. Chem.* **2003**, *42*, 2197.
- (12) Wisnubroto, D. S.; Nagasaki, S.; Enokida, Y.; Suzuki, A. *J. Nucl. Sci. Technol.* **1992**, *29*, 263.
- (13) Nagasaki, S.; Kinoshit, K.; Enokida, Y.; Suzuki, A. *J. Nucl. Sci. Technol.* **1992**, *29*, 1100.
- (14) Chmutova, M. K.; Kulyako, Y. M.; Litvina, M. N.; Malikov, D. A.; Myasoedov, B. F. *Radiochemistry* **1998**, *40*, 247.
- (15) Litvina, M. N.; Chmutova, M. K.; Myasoedov, B. F.; Kabachnik, M. I. *Radiochemistry* **1996**, *38*, 494.
- (16) Chmutova, M. K.; Litvina, M. N.; Pribylova, G. A.; Nesterova, N. P.; Klimenko, V. E.; Myasoedov, B. F. *Radiochemistry* **1995**, *37*, 396.
- (17) Chaumont, A.; Wipff, G. *Phys. Chem. Chem. Phys.* **2006**, *8*, 494.
- (18) Klamt, A.; Schüürmann, G. *J. Chem. Soc., Perkin Trans.* **1993**, *2*, 799.
- (19) Ehlers, A. W.; Frenking, G. *J. Am. Chem. Soc.* **1994**, *116*, 1514.
- (20) Delly, B.; Wrinn, M.; Lüthi, H. P. *J. Chem. Phys.* **1994**, *100*, 5785.
- (21) Li, J.; Schreckenbach, G.; Ziegler, T. *J. Am. Chem. Soc.* **1995**, *117*, 486.
- (22) Jonas, V.; Thiel, W. *J. Chem. Phys.* **1995**, *102*, 8474.
- (23) Schreckenbach, G.; Hay, P. J.; Martin, R. L. *J. Comput. Chem.* **1999**, *20*, 70.
- (24) Kaltsoyannis, N. *Chem. Soc. Rev.* **2003**, *32*, 9.
- (25) Vallet, V.; Macak, P.; Wahlgren, U.; Grenthe, I. *Theor. Chem. Acc.* **2006**, *115*, 145.
- (26) Becke, A. D. *J. Chem. Phys.* **1993**, *98*, S648.
- (27) Lee, C.; Yang, W.; Parr, R. G. *Phys. Rev. B* **1988**, *37*, 785.
- (28) Lan, J. H.; Shi, W. Q.; Yuan, L. Y.; Zhao, Y. L.; Li, J.; Chai, Z. F. *Inorg. Chem.* **2011**, *50*, 9230.
- (29) Lan, J. H.; Shi, W. Q.; Yuan, L. Y.; Feng, Y. X.; Zhao, Y. L.; Chai, Z. F. *J. Phys. Chem. A* **2012**, *116*, 504.
- (30) Lan, J. H.; Shi, W. Q.; Yuan, L. Y.; Li, J.; Zhao, Y. L.; Chai, Z. F. *Coord. Chem. Rev.* **2012**, *1406*.
- (31) Kuchle, W.; Dolg, M.; Stoll, H.; Preuss, H. *J. Chem. Phys.* **1994**, *100*, 7535.
- (32) Cao, X.; Dolg, M. *J. Mol. Struct. (THEOCHEM)* **2004**, *673*, 203.
- (33) Dolg, M.; Stoll, H.; Preuss, H. *J. Chem. Phys.* **1989**, *90*, 1730.
- (34) Vetere, V.; Maldivi, P.; Adamo, C. *J. Comput. Chem.* **2003**, *24*, 850.
- (35) Santo, E.; Di, Santos, M.; Michelini, M. C.; Marcalo, J.; Russo, N.; Gibson, J. K. *J. Am. Chem. Soc.* **2011**, *133*, 1955.
- (36) Michelini, M. D.; Russo, N.; Sicilia, E. *J. Am. Chem. Soc.* **2007**, *129*, 4229.
- (37) Frisch, M. J.; Trucks, G. W.; Schlegel, H. B.; Scuseria, G. E.; Robb, M. A.; Cheeseman, J. R.; Montgomery, J. A., Jr.; Vreven, T.; Kudin, K. N.; Burant, J. C.; Millam, J. M.; Iyengar, S. S.; Tomasi, J.; Barone, V.; Mennucci, B.; Cossi, M.; Scalmani, G.; Rega, N.; Petersson, G. A.; Nakatsuji, H.; Hada, M.; Ehara, M.; Toyota, K.; Fukuda, R.; Hasegawa, J.; Ishida, M.; Nakajima, T.; Honda, Y.; Kitao, O.; Nakai, H.; Klene, M.; Li, X.; Knox, J. E.; Hratchian, H. P.; Cross, J. B.; Bakken, V.; Adamo, C.; Jaramillo, J.; Gomperts, R.; Stratmann, R. E.; Yazyev, O.; Austin, A. J.; Cammi, R.; Pomelli, C.; Ochterski, J. W.; Ayala, P. Y.; Morokuma, K.; Voth, G. A.; Salvador, P.; Dannenberg, J. J.; Zakrzewski, V. G.; Dapprich, S.; Daniels, A. D.; Strain, M. C.; Farkas, O.; Malick, D. K.; Rabuck, A. D.; Raghavachari, K.; Foresman, J. B.; Ortiz, J. V.; Cui, Q.; Baboul, A. G.; Clifford, S.; Cioslowski, J.; Stefanov, B. B.; Liu, G.; Liashenko, A.; Piskorz, P.; Komaromi, I.; Martin, R. L.; Fox, D. J.; Keith, T.; Al-Laham, M. A.; Peng, C. Y.; Nanayakkara, A.; Challacombe, M.; Gill, P. M. W.; Johnson, B.; Chen, W.; Wong, M. W.; Gonzalez, C.; Pople, J. A. *Gaussian 03*, revision C.01; Gaussian, Inc.: Wallingford, CT, 2004.
- (38) Papas, B. N.; Schaefer, H. F. *J. Mol. Struct. (THEOCHEM)* **2006**, *768*, 175.
- (39) Frisch, M. J.; Trucks, G. W.; Schlegel, H. B.; Scuseria, G. E.; Robb, M. A.; Cheeseman, J. R.; Scalmani, G.; Barone, V.; Mennucci, B.; Petersson, G. A.; Nakatsuji, H.; Caricato, M.; Li, X.; Hratchian, H. P.; Izmaylov, A. F.; Bloino, J.; Zheng, G.; Sonnenberg, J. L.; Hada, M.; Ehara, M.; Toyota, K.; Fukuda, R.; Hasegawa, J.; Ishida, M.; Nakajima, T.; Honda, Y.; Kitao, O.; Nakai, H.; Vreven, T.; Montgomery, J. A., Jr.; Peralta, J. E.; Ogliaro, F.; Bearpark, M.; Heyd, J. J.; Brothers, E.; Kudin, K. N.; Staroverov, V. N.; Kobayashi, R.; Normand, J.; Raghavachari, K.; Rendell, A.; Burant, J. C.; Iyengar, S. S.; Tomasi, J.; Cossi, M.; Rega, N.; Millam, J. M.; Klene, M.; Knox, J. E.; Cross, J. B.; Bakken, V.; Adamo, C.; Jaramillo, J.; Gomperts, R. E.; Stratmann, O.; Yazyev, A. J.; Austin, R.; Cammi, C.; Pomelli, J. W.; Ochterski, R.; Martin, R. L.; Morokuma, K.; Zakrzewski, V. G.; Voth, G. A.; Salvador, P.; Dannenberg, J. J.; Dapprich, S.; Daniels, A. D.; Farkas, O.; Foresman, J. B.; Ortiz, J. V.; Cioslowski, J.; Fox, D. J. *Gaussian 09*, revision A.02; Gaussian, Inc.: Wallingford, CT, 2009.
- (40) Wiberg, K. B. *Tetrahedron* **1968**, *24*, 1083.
- (41) Carpenter, J. E.; Weinhold, F. *J. Mol. Struct. (THEOCHEM)* **1988**, *169*, 41.
- (42) Foster, J. P.; Weinhold, F. *J. Am. Chem. Soc.* **1980**, *102*, 7211.
- (43) Reed, A. E.; Weinstock, R. B.; Weinhold, F. *J. Chem. Phys.* **1985**, *83*, 735.
- (44) Reed, A. E.; Curtiss, L. A.; Weinhold, F. *Chem. Rev.* **1986**, *6*, 899.
- (45) Becke, A. D. *Phys. Rev. A: At, Mol., Opt. Phys.* **1988**, *38*, 3098.
- (46) Perdew, J. P. *Phys. Rev. B* **1986**, *33*, 8822.
- (47) Allen, P. G.; Bucher, J. J.; Shuh, D. K.; Edelstein, N. M.; Reich, T. *Inorg. Chem.* **1997**, *36*, 4676.
- (48) Dalley, B. N.; Mueller, M. H.; Simonsen, S. H. *Inorg. Chem.* **1971**, *10*, 323.
- (49) Hay, P. J.; Martin, R. L.; Schreckenbach, G. *J. Phys. Chem. A* **2000**, *104*, 6259.
- (50) Takano, Y.; Houk, K. N. *J. Chem. Theory Comput.* **2005**, *1*, 70.
- (51) Schreckenbach, G.; Shamov, G. A. *Acc. Chem. Res.* **2010**, *43*, 19.
- (52) Shamov, G. A.; Schreckenbach, G. *J. Phys. Chem. A* **2005**, *109*, 10961.
- (53) Grigor'ev, M. S.; Charushnikova, I. A.; Krot, N. N.; Yanovskii, A. I.; Struchkov, Yu. Y. *Zh. Neorg. Khim.* **1994**, *39*, 179.
- (54) Schulza, W. W.; Horwitz, E. P. *Sep. Sci. Technol.* **1988**, *23*, 1191.